Journal of CO2 Utilization 92 (2025) 103024

Contents lists available at ScienceDirect

Journal of CO2 Utilization

journal homepage: www.elsevier.com/locate/jcou

# Capturing microalgae within aerosols provides carbon capture bio-functionality

Elbaraa Elghazy [a,c], Matt M.J Davies [b], Nicholas T.H Farr [a,d], Cornelia Rodenburg [a,d], Jon R. Willmott [b], Jagroop Pandhal [a,*]

[a] School of Chemical, Materials and Biological Engineering, The University of Sheffield, Sheffield, United Kingdom
[b] School of Electronic and Electrical Engineering, The University of Sheffield, Sheffield, United Kingdom
[c] Department of Construction and Building Engineering, Arab Academy for Science, Technology, and Maritime Transport, Cairo, Egypt
[d] Insigneo Institute for in silico Medicine, University of Sheffield, Sheffield, United Kingdom

ARTICLE INFO

*Keywords:*
Aerosol
$CO_2$ Capture
Industrial emissions
Microalgae
Carbon sequestration
Sustainable technology
Greenhouse gas reduction
Climate change mitigation

ABSTRACT

Climate change due to the greenhouse effect poses arguably the greatest challenge to humanity. Addressing the sources of $CO_2$ and reducing current atmospheric levels is the paramount task for scientists and engineers. Carbon capture with storage or utilization technologies are key to achieving this goal. Biological carbon fixation is an effective method of converting pollutant $CO_2$ into usable biochemicals for industrial applications. Inspired by recent evidence that 95 % of $CO_2$ from aerosol emissions from an Australian forest fire was captured by algae in the Southern Ocean, as well as the ability of algae to be transported within aerosols, we propose a novel technique for $CO_2$ sequestration based on creating aerosols containing metabolically active cyanobacteria. Using aerosols as a microenvironment for *Synechocystis* cells enables a significant increase in gas-liquid-interfacial-surface-area while reducing the volume of water required. We utilize electron microscopy and hyperspectral microscopy to assess the effects of aerosolization and high $CO_2$ concentrations on microbial cell viability. Additionally, we implemented highspeed imaging and oil immersion microscopy to determine the effectiveness of the aerosolization technique for forming aerosols and optimizing process parameters. We show that 1 % $CO_2$ (v/v) is ideal for $CO_2$ capture, where cell stress was minimized. Using cell densities of $1.2 \times 10^8$ cell/mL was the most efficient in terms of the number of cells aerosolized when compared to the input cell density. We report a 6-fold increase in carbon fixation rates ($gCO_2\ g^{-1}$ biomass $hr^{-1}$) over alternative popular cultivation techniques such as bubble columns.

## 1. Introduction

The effects of climate change, driven by $CO_2$ greenhouse gas emissions poses a persistent and ever-increasing threat to our continued way of life [1–4]. The relationship between $CO_2$ in the atmosphere and the changing climate are well documented [5,6] and the work to both reduce $CO_2$ emission rates and reduce existing atmospheric $CO_2$ levels has become increasingly important. Efforts to reduce $CO_2$ emissions include novel technologies to capture gases from industrial processes. Carbon capture and storage (CCS) is the conversion of $CO_2$ to storable materials [1,7]. CCS techniques include physical adsorption techniques, wherein solid materials like zeolites or metal-organic frameworks act as $CO_2$ sorbents. Additionally, physical methods such as membrane separation technologies have gained prominence, permitting the selective passage of $CO_2$ molecules through specialized membranes[8–10]. Carbon mineralization processes implement the natural geological sequestration of $CO_2$, while direct air capture techniques involve physically removing $CO_2$ from the atmosphere and are gaining increasing attention [11–15]. Chemical absorption involves the use of liquid solvents to capture $CO_2$, a process commonly employed in post-combustion carbon capture systems [16,17]. Further to CCS is carbon capture and utilization (CCU), whereby $CO_2$ is converted into useful materials that can then be utilized for other purposes [18]. Some of the CCS techniques described above, such as carbon mineralization, can produce $CaCO_3$ for instance [12,13,15], which is widely utilized as an additive in cement, one of the most fundamental materials in modern civilization [19,20].

Biological $CO_2$ fixation has gained traction as a CCU technology that enables the conversion of $CO_2$ into biomass. This biomass is then

* Corresponding author.
*E-mail address:* j.pandhal@sheffield.ac.uk (J. Pandhal).

https://doi.org/10.1016/j.jcou.2025.103024
Received 10 October 2024; Received in revised form 11 December 2024; Accepted 13 January 2025

available to be harvested and biochemicals extracted so they can be utilized as materials, fertilizer or even food [21,22]. $CO_2$ can be directly fixed by autotrophs such as trees in forests or algae in the ocean, through photosynthesis. Although rainforests garner significant media attention in terms of storage of carbon, a far more significant "carbon sink" exists in the oceans. 10 % of ocean biomass is accounted for by microalgae and macroalgae [23] and 50 % of global oxygen is produced through algal primary production [24]. The potential to capture $CO_2$ with photosynthetic microorganisms has led to increased interest from industry. For example, in the steel industry, approximately 2 tons of CO2 is released per ton of steel produced, and over 1.8 bn tons is produced annually to maintain our modern lifestyles [25,26]. The capture of industrial $CO_2$ by using algae has been researched predominantly by bubbling gaseous effluents into aquatic-based photobioreactors (PBRs), such as bubble columns [27], where algae are suspended in a growth medium. Algae can take up $CO_2$ directly or as $HCO_3^-$, depending on the strain and physiological conditions [28]. The surface area of the bubbles, referred to as the gas-liquid interfacial surface area (GLISA), will affect overall mass transfer and hence, algal growth rates and $CO_2$ capture rates. The surface area and volume of a sphere are proportional to the square and cube of the radius respectively, and so minimizing the size of the bubbles significantly increases the ratio of $CO_2$ that is available to the algae compared to the total volume of $CO_2$ passing through the column. Maximizing the GLISA can be accomplished through using microbubbles, where the $CO_2$ passes through a bubbling element such as a venturi microbubble generator [29] or fluidic oscillators [30], which forms the $CO_2$ stream into microbubbles of diameter of less than one millimeter.

A significant drawback of algae-based $CO_2$ sequestration is the limited scalability. Large open ponds and PBRs are required, [27], requiring large quantities of water. Although specific concentrations of $CO_2$ are introduced into the PBRs, most of the gas is lost into the headspace and therefore recycling is often required. Although bubbling in higher $CO_2$ concentrations would appear to be more amenable for industrial gaseous effluents, this drastically reduces the pH of the medium to toxic levels. One technique to address this while also increasing the contact surface area between the algal cells and $CO_2$, is immobilization-based CCU, where algal cells are adhered to a solid scaffold. In a novel approach, In-na et al. (2020) demonstrated this technique by cultivating cells onto high surface area loofah sponges with a latex binder [31]. However, this method directly exposes cells in biofilms to high external $CO_2$ concentrations, that can lead to stress conditions. Moreover, maintaining moist conditions can be a challenge when scaling such a system.

To overcome these challenges, we propose an entirely new method for algal-CCU that exploits current particulate reduction technology based on aerosolization. We designed a technique for biologically activating the aerosols, to add carbon capture bio-functionality. By aerosolizing algal cell suspensions for the purpose of $CO_2$ sequestration, we aimed to exploit the enhanced GLISA of aerosols (Fig. 1). This new approach was inspired by the current use of aerosols in industries for capturing gases and particulate matter, and hence has already been scaled to commercial levels. According to literature, creating biologically active aerosols as a beneficial process has never been undertaken previously. Yet, this technology could dramatically increase the surface area over which a gas – cell membrane interaction could occur, reducing the volume of biomass required for an equivalent $CO_2$ capture rate. Since the first indication that "bioaerosols" exist in nature, attention has largely been directed towards understanding their impacts on human health, and the mechanisms of emissions to the atmosphere, recently reviewed by *et al.* and Yong Le Pan et al. [32,33]. Although it is known that toxins from specific algal strains can also be transported within sea spray aerosols over large distances[34], recent evidence has shown that whole algal cells can also be transported, reaching densities of $10^{-4}$ to $10^4$ cells/$m^3$ [35]. The concept of linking large scale $CO_2$ capture with algal bloom generation was inspired by natural aerosols. It was calculated that during the Australian wildfire seasons in 2019 and 2020, covering 28,570 square miles, led to the release of 715 teragrams of $CO_2$. Remarkably, an estimated 95 % of this was captured by resulting phytoplankton blooms downwind in the Southern Ocean [36].

Our study utilizes surface acoustic waves (SAW) to aerosolize cell suspensions containing prokaryotic algae (cyanobacteria) for carbon capture. We performed a series of experiments with high-speed imaging to evaluate parameters such as cell density on effective aerosolization. A new aerosolization system was designed to quantify $CO_2$ removal in a batch system. We subsequently used secondary emission hyperspectral imaging (SEHI) and visible/near infrared hyperspectral microscopy to analyze the effects of elevated $CO_2$ concentrations on aerosolized algal cells, an abiotic stress on microbial cells that has not been investigated previously. We showcase for the first time how biologically activated

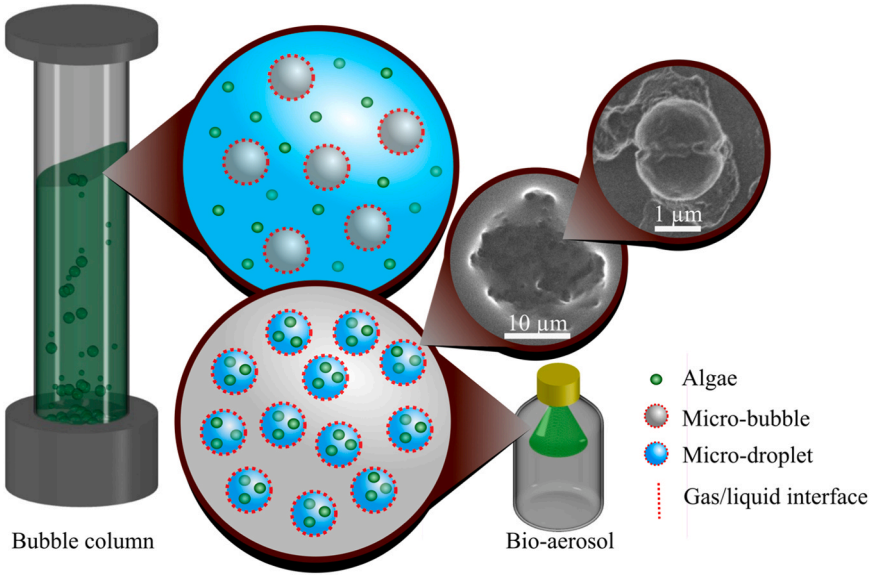


**Fig. 1.** A diagram comparing microbubbles and microdroplets for carbon sequestration through $CO_2$ fixation. The gas liquid interfacial surface area is highlighted to emphasize the equivalence between both techniques for orders of magnitude reduction in liquid volume. SEM micrographs of an algae-entrained micro-droplet and an algae cell are shown.

aerosols enable the capture of industrial greenhouse gases as a new engineering approach that once optimized and scaled, has the potential to lead to significant environmental benefits.

## 2. Methodology

To investigate the effectiveness of biologically activating aerosols, the experimental strategy was devised into three key aspects: aerosol formation and optimization, assessing the health of the algae post-process, and finally, $CO_2$ capture measurements.

## 3. Aerosolization apparatus and algae selection

The method of aerosolization was selected to produce the smallest droplets possible that could still viably contain algae. Aerosols were formed by contact between a liquid reservoir and a round, perforated metal membrane, actuated by a piezo element. The membrane vibrates at high frequency when the piezo element is powered forcing the liquid through the perforations (5 μm in diameter) forming tiny droplets. Droplets of this size can be produced with nozzles, analogous to the nozzles used in industrial applications for dust suppression. The method was selected here due to the ease of incorporating it at small scales for the experimental setup.

*Synechocystis* sp. PCC 6803 (herein referred to as *Synechocystis*) was chosen because the cells have a relatively small diameter (2–5 μm) and so they could be entrained within the microdroplets of the selected aerosol size. *Synechocystis* stock cultures were grown in a 500 mL flask containing BG11 medium in an Algem photobioreactor (Algenuity, UK). The temperature was maintained at 32 ℃, with continuous mixing at 120 rpm and illuminated with light of 500 μmol photons $m^{-2}s^{-1}$. The pH of the culture was maintained at 9 using intermittent doses of $CO_2$ to ensure optimal growth conditions. Two-thirds of the cyanobacteria culture was removed every three days and replaced with fresh media to maintain a continuous culture. It was anticipated that there would be a reduction in cell density due to the aerosolization process. The small perforations in the metal membrane blocked some of the algae. It was necessary to calibrate this effect so optimal parameters could be selected for the $CO_2$ capture experiment and to remove bias due to our selected method of aerosolization. Other fine aerosolization techniques, such as spray nozzles, would have a similar effect due to prefilters built into the nozzles and so would need to be similarly calibrated.

The cyanobacteria cells were diluted to different densities. Cell densities of $4 \times 10^7$, $8 \times 10^7$, $1.2 \times 10^8$ and $1.6 \times 10^8$ cell/mL at a volume of 50 mL were aerosolized using the piezoelectric atomizer into the 10 L chamber for a duration of 15 minutes. Following this aerosolization process, the resulting aerosols were allowed to settle for a period of 30 minutes. After the settling period, the cell density of the settled algae was measured. Each experiment was performed in triplicate. The aerosolization efficiency (AE) was determined by dividing the cell density of collected cell suspension after aerosolization by the initial cell density suspension used.

After optimizing the aerosolization parameters, it was necessary to ensure that there were algae cells within the aerosols, and to assess the influence of input cell density on droplet cell density. Secondly, it was required to measure the droplet sizes to calculate the surface area per-unit-volume and quantify the effect of input cell density on droplet size. It was hypothesized that the increased viscosity due to higher cell density might affect droplet size. Two methods were employed to image the droplets to address the challenges, static and dynamic. Static imaging was used to obtain images of cells that were contained within droplets. To achieve this, cyanobacteria cultures were aerosolized, and the resulting droplets were allowed to fall upon a thin layer of silicon oil. The cultures used in the experiment had varying cell densities, of $1.6 \times 10^8$, $3.2 \times 10^8$ and $3.2 \times 10^9$ cell/mL to assess whether a large increase in cell density would produce droplets with a proportional increase in cell density. The oil-immersed droplets were imaged using an optical microscope. This allowed for detailed observations of the cells contained within the droplets. The droplets were deformed from their spherical shape in the oil [37], and so this method could not be used to measure the droplet sizes.

Dynamic imaging was used to measure the effect of input cell density on droplet size. A high-speed camera (Hamamatsu Orca flash 4.0, Japan) attached to an optical microscope, to capture a video of the process. A small funnel was placed on top of the microscope lens to focus a small amount of the aerosol for imaging. The aerosol droplets could then be imaged directly. This was done for deionised (DI) water as well as algae cultures with different cell densities of $1.6 \times 10^8$, $3.2 \times 10^8$ and $3.2 \times 10^9$ cell/mL. The video was divided into individual frames and sorted into images that contained in-focus images of the droplets, which were then used to measure the distribution of droplet sizes for each cell density. The effective pixel resolution was calibrated with a target of known dimensions to convert from size in pixels to μm.

## 4. Algae health measurement

As it is not known how elevated levels of $CO_2$ affect the algae contained within microdroplets, an experiment was designed to measure the change in pH in the algae media with increasing $CO_2$ concentration. The parameters were maintained to simulate the experimental conditions for quantifying the $CO_2$ capture to ensure consistency. Algae cell suspensions were aerosolized into a preconditioned chamber of selected $CO_2$ concentrations (0.04 %, 1 % and 5 % v/v) after which the change in pH of the settled cell suspension was measured. The change in cell density, corrected for AE, was also measured to assess the effect of the $CO_2$ concentrations on the collected cells.

Visible hyperspectral microscopy, scanning electron microscopy (SEM) and secondary electron hyperspectral imaging (SEHI) were also used to assess the impact of the high levels of $CO_2$ on the algae. Hyperspectral images were taken of the algae using a Nikon TS100 microscope adapted for hyperspectral imaging using a custom, modular system previously demonstrated by Stuart et al. [38], [39]. Algae were aerosolized in a glass chamber with a controlled $CO_2$ level for 5 minutes and were then left in the $CO_2$ atmosphere for a further 5 minutes. A sample of the algae solution was then taken from the chamber and placed on a glass slide and imaged with hyperspectral system over a wavelength range of 480–700 nm.

The cell health could then be determined using Eq. 1:

$$G = \frac{\lambda_{554}}{\lambda_{677}} \tag{1}$$

Where G is referred to as the greenness index [40], $\lambda_{554}$ and $\lambda_{677}$ are the spectral transmission measured at 554 nm and 677 respectively. Chlorophyll is spectrally characterised by strong absorption in the blue and red portions of the visible spectrum with a significant increase in transmission/reflection towards the near infrared, referred to as the “red edge” [41]. This spectral characteristic is affected when organisms containing Chlorophyll are stressed and the red strong absorption in the red is reduced thereby providing a means of assessing the relative effect of elevated $CO_2$ on the algae.

Images of the algae cells in the droplets and in isolation were captured using SEM, and then spectra of the algae were measured using SEHI. SEHI is an innovative characterization technique employed within an SEM chamber, providing nanometer-depth sampling. Its surface sensitivity yields spectra, offering chemical bonding information, and highly resolved chemical maps. Past studies attest to SEHI’s efficacy in mapping functional groups on polymers [42,43].

Live cellular imaging of the algae droplets was performed within a FEI Helios Nanolab G3 (FEI Company, USA) microscope via the application of NanoSuit®, its use to visualize live specimens within an SEM has been described previously [44]. Biologically active aerosols were sprayed onto an aluminum SEM stub, 10 μL of NanoSuit® solution was

then pipetted onto the stub covering the dispensed algae film. Prior to use, the SEM stub had been coated with aluminum foil and exposed low-pressure air glow discharge in a Diener Electronic Zepto plasma cleaner at 40 kHz, 100 W, and 0.3 mbar air for 5 minutes. The Nano-Suit® layer, containing algae droplets, was then polymerized by a 5 kV electron beam before low-voltage SEM imaging was conducted. An accelerating voltage of 1 keV at typical chamber vacuum pressures in the range of 10 −6 mbar and a working distance of 4 mm were chosen to avoid sample damage through surface charging. An Everhart-Thornley Detector (ETD) was selected for low magnification SE images and a Through Lens Detector (TLD) for high magnification SE images. SEHI data acquisition was undertaken as described previously [45,46]. SEHI generation was performed using the Helios Nanolab G3 operating conditions of 1 keV (monochromated) and 50 pA immersion mode (mode II/UHR). This microscope can provide ultra high-resolution images at voltages $< 1$ keV. To ensure that images were taken of the true algae surface, no conductive coating was applied to the samples in contrast to typical SEM analysis practice. A vacuum pressure of ~10 −6 mbar was maintained at a working distance of 4 mm. The collection of SEHI of different energy ranges was enabled through the adjustment of the mirror electrode voltage (MV) together with a tube bias setting of 150 V. Stepping the MV in a range of −15 to 15 V was achieved through the use of an automatic iFast collection recipe [46]. All images were acquired at a frame interval of 0.5 s and an MV step size of 0.5 V, corresponding to an electron energy step size of about 0.2 eV. Image processing was done with Fiji ImageJ software (ImageJ2, National Institute of Health, USA).

## 5. $CO_2$ capture measurement apparatus

A batch airtight experimental setup (Fig. 2) was designed to quantify the effectiveness of biologically active aerosols for $CO_2$ capture. $CO_2$ and air taps were connected to flow meters, to allow control of the relative quantities of the gases and desired $CO_2$ concentrations were introduced into the mixer followed by the inlet sensor. The gas was supplied through the clear glass chamber (10 L Duran bottle) and passed through the outlet sensor. The chamber was illuminated throughout the experiment using a near light source that provide 3500 lumens. Valves were used to close the system once the required $CO_2$ levels inside the chamber were achieved. $CO_2$ levels were monitored with optical $CO_2$ sensors (CO2meter, USA). A hand bulb pump was used to circulate the gas in the system.

The $CO_2$ capture experiment comprised three stages. Initially, the $CO_2$ (v/v) concentration inside the gas-tight chamber was elevated to the required level and monitored using the inlet and outlet sensors; sealing the inlet and outlet tap when both sensors' readings were the same ($CO_{2Pre}$). The aerosols were introduced in the second phase using the top atomizer unit where algae were kept in a closed vessel. Aerosols were produced continuously for 40 minutes, and then allowed to settle for 30 minutes. Finally, the gas was circulated using a hand bulb pump for the $CO_2$ measurement ($CO_{2Post}$). The percentage of captured $CO_2$ was calculated using Eq. 1:

$$\text{Removal\%} = \frac{CO_{2Pre} - CO_{2Post}}{CO_{2Pre}} \bullet 100 \quad (2)$$

$CO_2$ measurements were undertaken with no aerosols added, aerosolization with DI water only and with *Synechocystis* cells added. We also performed the latter experiment with the photosynthetic inhibitor methyl viologen added to the bottom of the aerosolization chamber to eliminate carbon fixation from cells that have collected at the bottom.

## 6. Results and discussion

The results are presented and discussed in three subsections: a focus on optimizing process parameters to create aerosols containing algae, the impact of $CO_2$ on the entrained algae, and finally, quantification of $CO_2$ removal within the system.

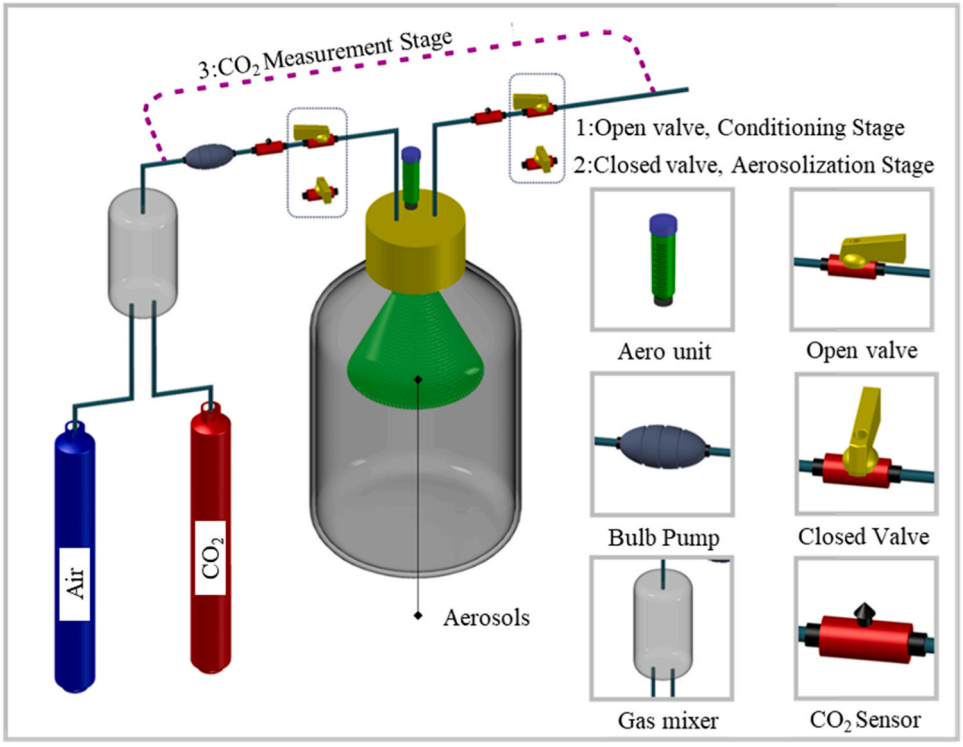


**Fig. 2.** The three stages of the measurement process are shown. In the first stage, The inlet and outlet valves are both open and the $CO_2$ concentration is monitored until the desired level is achieved. During stage two, the valves are closed and the aerosols are produced inside the chamber for 40 minutes. The resulting $CO_2$ concentration is measured in stage 3 by circulating the air inside the chamber through the sensors without introducing new gas from outside.

## 7. Biologically active aerosol optimisation

It was hypothesized that algal cell density would impact on how many cells were aerosolized within our system. Therefore, AE was calculated at four different cell densities (Fig. 3). The results show the maximum AE was 45 %, with no significant proportional decrease in AE for cell densities less than of $1.2 \times 10^8$ cell/mL. However, the AE value dropped significantly when the cell density increased to $1.6 \times 10^8$ cell/mL, indicating an optimum cell density of $1.2 \times 10^8$, where the greatest number of cells are aerosolized when compared to the input cell density. Differences in AE were statistically significant between all cell densities except between the $4.0 \times 10^7$ and the $1.2 \times 10^8$ cell/mL.

This result provided an ideal cell density that would be used for the subsequent $CO_2$ capture measurements. However, AE would be process-dependent and would need to be quantified for other aerosolization techniques. The analysis of AE suggested that cells were being passed through the piezo-actuated membrane and collected in the bottom of the aerosolization chamber. However, this did not guarantee that cells were entrained in the aerosolized droplets. Fig. 4 shows images of the cells captured within the droplets from the oil immersion tests described in the section 3.1.

Cells can be seen within the droplets immersed in the silicone oil. This confirmed that cells were present in the aerosols. The process was repeated for increasing cell density up to $3.2 \times 10^9$ cell/mL to qualitatively assess whether cell densities in the droplets increased accordingly. Since this method of capturing droplets in silicone oil may affect the visibility of cells within individual droplets, quantitative analysis was not performed on this data to reveal how many droplets actually contained algal cells. There was an implied increase in droplet cell density, but it was deemed to not be significant enough to warrant increasing the cell density for the $CO_2$ capture experiment given the drop in AE with increasing cell density.

Measurement of the surface area of the droplets was necessary to rigorously parameterize the aerosolization method selected for this work. We initially aerosolized water containing no algae and a cell suspension with cell density of $1.6 \times 10^8$ cell/mL to measure the droplet size and to see if the algae influenced the droplet formation. However, it could be seen in the images that there seemed to be smaller (<2 μm) particles in the algae solution that were not present when only water was aerosolized. We hypothesized that these were "detached" cells, independent of droplets. We aerosolized increasing cell densities up to $3.2 \times 10^9$ cell/mL to test this hypothesis. Fig. 5A-C shows the experimental setup as well as images of a droplet and a detached cell.

Fig. 5D shows a graph of droplet size against increasing cell density. Increasing the cell density did not affect the droplet size. However, detached cells are observed in samples containing algae in aerosols. Although it is possible that the cells were detached due to drying of the aerosol, the experiments were undertaken at room temperature, hence it was deemed unlikely.

## 8. Effect of $CO_2$ on algae

Measuring the cell density and pH of the cell suspensions in the well of the aerosolization chamber in different $CO_2$ concentrations provided insight into understanding how algae health was impacted by increasing the concentrations of $CO_2$ (Fig. 6).

After 15 minutes of aerosolization, there was a 19 % reduction in cell density upon elevating $CO_2$ from concentrations in air (0.04 %) to 1 % (v/v) $CO_2$, and an additional 24.5 % decrease upon elevation of $CO_2$ concentrations to 5 % (v/v). We hypothesize that the rapid decrease in cell count could be attributed to a simultaneous drop in pH as depicted in Fig. 6 (pH was as low as 6.7). This could also be due to the toxicity caused by high levels of $CO_2$, or a combination of the two. The effect of elevated $CO_2$ levels on various species of algae has previously been investigated [47,48], mostly introduced through bubbling air mixed with $CO_2$ into the cell suspension. In a study undertaken in 2020, algal photosynthetic activity declined at 10 % (v/v) $CO_2$ concentration with complete inhibition of cell growth at 15 % (v/v) $CO_2$, which illustrates the toxic effects of elevated $CO_2$ concentration on algae cells [49]. Although these systems provide specific levels of $CO_2$ in the input gas, they are impacted by other important parameters, such as the flowrate of gas introduced and the size of bubbles; both of which would have a significant effect on the mass transfer of gas to liquid. Moreover, cells are not exposed directly to these $CO_2$ concentrations because most of the gas is released into the headspace when bubbles reach the surface of the aqueous phase in PBRs. In our study, aerosols containing *Synechocystis* cells required a total volume of 5 mL of cell suspension to fill a 10 L chamber containing a specific $CO_2$ concentration, meaning that each aerosol droplet is directly exposed to the measured $CO_2$ concentration within the chamber. We presumed this would have more instantaneous effects on cell viability. Here, the impact of elevated levels of $CO_2$ on cell viability was quantified by measuring the cell density after aerosolization. To further understand the impact of elevated levels of $CO_2$ on cell viability beyond what proportion of cell survived, we applied visible

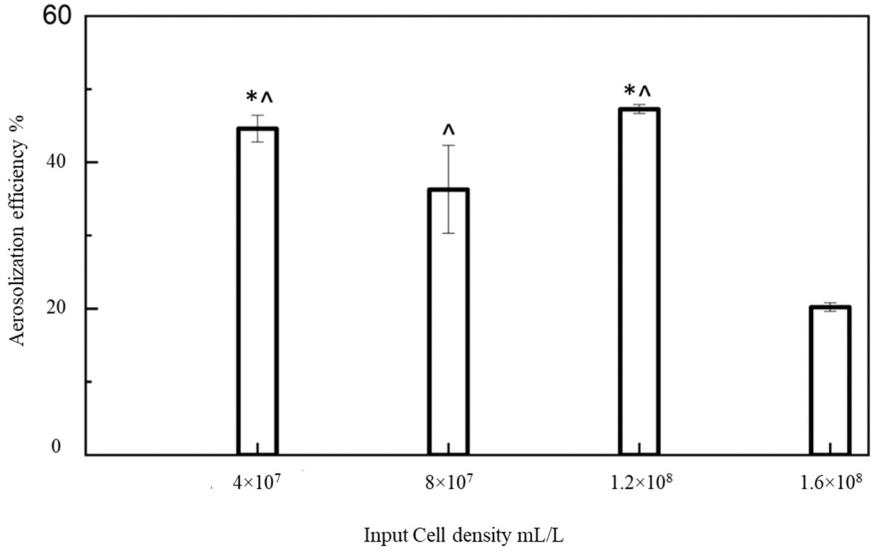


**Fig. 3.** Aerosolization efficiency calculated as a factor of increasing cell density.[*significantly different from $8.0 \times 10^7$, ^ significantly different from $1.6 \times 10^8$ using ANOVA with Tukey postHoc test].

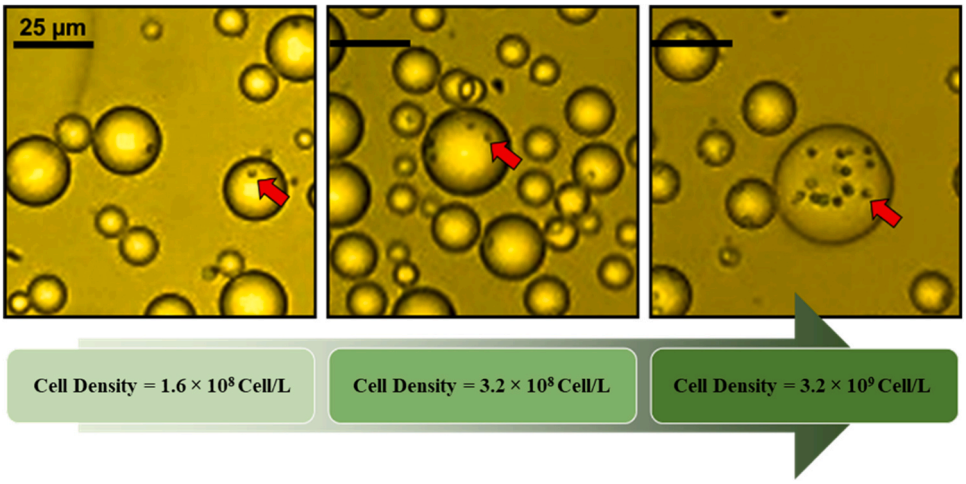


**Fig. 4.** Micrographs of algae entrained microdroplets imersed in silicone oil with increasing inoculum cell density. Algae cells can be seen within the droplets, however, the size bars do not represent accurate aerosol sizes as they are laying across a silicone surface.

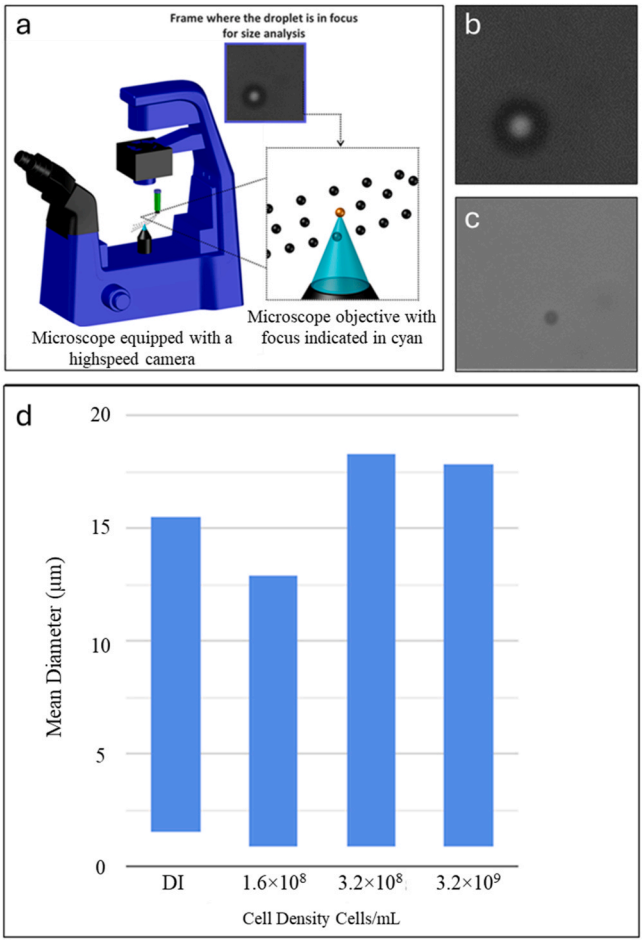


**Fig. 5.** (a) The experimental setup for dynamic imaging of the micro-droplets; (b) A micrograph of a droplet in air; (c) A micrograph of a detached cell in air; (d) A graph showing droplet diameter range when increasing cell density.

hyperspectral microscopy analysis. This enabled a cell-wise view of the health of the algae, where cell health could be determined for the living cells. Hyperspectral images of all living cells for the three $CO_2$ concentrations were calculated (Fig. 7).

By measuring the spectral transmission of aerosolized cells, we calculated a greenness index, implying Chlorophyll *a* content (Fig. 7). There was a clear increase in spectral transmission at 677 nm, indicative of reduced Chlorophyll *a*, and potentially cell health.

We then further investigated the cell health in response to $CO_2$ by directly imaging the cells using SEM and measuring their secondary electron spectra with SEHI (Fig. 8).

Capturing data in this way provides insights into the chemical structure of the algae cells. Variation in cellular structure are also visualizable in the SEM images in Fig. 8 B as $CO_2$ concentrations increase. In the spectral data (Fig. 8 A), a consistent peak around 0.8 eV is evident across all samples showing that peak position does not change in this energy range, and therefore acts as an internal reference peak. However, there is a shift in energy of the main peak (2.6–2.9 eV) as $CO_2$ concentrations increase from 0.04 % to 1–5 % (v/v). This implies a chemical change on the surface of *Synechocystis* cells. In 1 % $CO_2$, the peak is broadened, implying populations of cells with similar chemistry to those in 0.04 % $CO_2$, and 5 % $CO_2$. It is likely that this dynamic change in cell surface chemistry of *Synechocystis* cells could be due to the S-layer composition. *Synechocystis* consist of an outer membrane (~15 nm) and inner membrane (~10 nm), with the periplasmic space (15 nm) between them. Surrounding the outer membrane is the surface "S-layer" (~10 nm), made up of crystalline arrays of proteins covering the entire cell periphery [50]. Due to SEHI's sampling depth of $>$ 10 nm, the chemical information provided from SEHI is expected to be in response to the chemistry of this S-layer. When considering the SEHI images and spectra in combination, it is notable that the cells at 1 % $CO_2$ undergo a process of remodeling at the point where the chemical composition of the resulting S-layers is most variable. This study hypothesizes that the S-layer of cells exposed to 1 % $CO_2$ undergoes varying biogenesis processes, with some cells surviving and others dying. This hypothesis is supported by the observation that cells imaged at 5 % exhibited a more uniform chemical S-layer composition, showing a more homogeneous cell population. We do note here that cells which have died and lysed, may release enzymes that can capture $CO_2$ prior to degradation, as cell-free enzymatic systems.

## 9. Quantification of $CO_2$ capture

A batch aerosolization system was designed to allow quantification of $CO_2$ removal rates in response to introducing aerosols. This closed system enabled conditioning of the aerosolization chamber to the selected 1 % (v/v) $CO_2$ concentration, where algal health was deemed relatively unimpacted (Section 3.2). $CO_2$ was measured before and after 40 minutes of aerosolization. Four experimental conditions were tested (Fig. 9); no aerosolization, DI water aerosols and aerosols with algae

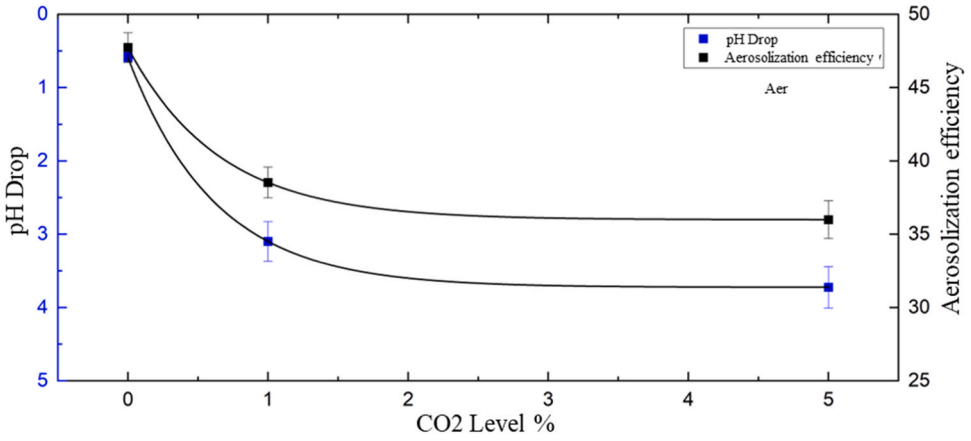


**Fig. 6.** A dual-axis graph showing pH drop (blue) and Aerosolization Efficiency (AE) (black) as $CO_2$ concentrations increase. There is a significant reduction in pH and AE from 0 % to 1 % v/v $CO_2$, however, the change from 1 % to 5 % v/v $CO_2$ is minimal.

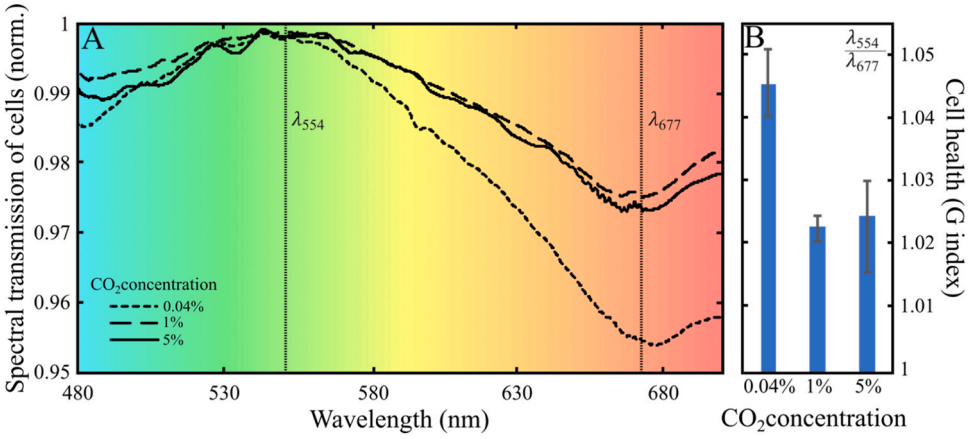


**Fig. 7.** (a) A graph of spectral transmission of algae cells exposed to 0.04, 1 and 5 % (v/v) $CO_2$ concentration. There is a characteristic dip at 680 nm, which is significantly reduced for elevated levels of $CO_2$, indicating the cell health is affected.

($4 \times 10^7$ cells/mL). The 'No aerosolization' step was performed to quantify any system losses, which was confirmed by no quantifiable change in $CO_2$ level at the beginning and end of the experiment (after 70 min). Aerosolization of DI water showed a small removal of approximately 2 % of initial $CO_2$, equivalent to 200 ppm over 40 min. This is expected due to the mass transfer of $CO_2$ to water droplets in a chamber that is saturated with $CO_2$, and was demonstrated previously [51]. $CO_2$ changes were calculated as percentage of removal (Fig. 9). To eliminate the potential of cells collected in the chamber well performing photosynthesis, fixing $CO_2$ and hence contributing to removal rates, the photosynthetic inhibitor, methyl viologen was added to the well and the latter experiment repeated (Fig. 9).

A 10 % reduction in $CO_2$ concentration in the chamber was achieved after 40 mins when biologically activated aerosols were applied with a starting concentration of 1 % (v/v) $CO_2$. This was assumed to be due to biological $CO_2$ fixation. When methyl viologen was added to the chamber, the reduction was not impacted. With the system conditions applied, $CO_2$ fixation rates were calculated at 3.52 g $CO_2$ $g^{-1}$ biomass $h^{-1}$. This data implies that algal cells can fix the $CO_2$ within the droplets with a much higher efficiency in comparison to alternative, algae-based $CO_2$ fixation techniques. This drastically exceeds traditional techniques using PBRs when considering time or quantity of resources used i.e., capital, water, nutrients and cell concentrations. It is important to measure actual $CO_2$ removal, rather than inferring from algal biomass accumulation, because this is a direct method of measurement [52]. In previous work, direct measurements using the microalga *Chlorella* in 250 mL flasks demonstrated $CO_2$ removal rates of 0.013 $gL^{-1}$ $hr^{-1}$, using 0.5–3 $gL^{-1}$ of algal biomass. This results in a removal rate range of 0.026 $gCO_2$ $g^{-1}$ biomass $hr^{-1}$ to 0.0041 $gCO_2$ $g^{-1}$ biomass $hr^{-1}$ [52]. A transition away from traditional PBRs has shown more promise due to the increased algal-gas surface area. For example, a carbon capture study utilizing immobilized cyanobacteria attached to bio-composite loofah sponges significantly outperformed PBRs, showing $CO_2$ fixation rates between 0.005–0.039 $gCO_2$ $g^{-1}$ biomass $hr^{-1}$, which is 5–10 times the rate of suspension experiments [31].

This new approach did expose algae to stressful conditions due to high amounts of $CO_2$ in the chamber and the large surface area to volume ratio of low μm diameter-range aerosols. At concentrations as high as 5 % $CO_2$ (v/v) we evidenced increased cell lysis, reduced chlorophyl *a* levels, and potentially stress-induced changes in algal S-layer proteins. Therefore, any integration of this technology would need to consider adjusting process conditions to reduce stress or exploit tolerant organisms. In terms of exploiting different microalgae, there are bioprospecting efforts to isolate strains that have high growth rates, and therefore will be able to fix $CO_2$ at higher rates. For example, there has been the recent exciting discovery of the cyanobacterium *Synechococccus* sp. PCC11901 with a doubling time of 2 hours [53], several fold faster than similar species. Considering the lifetime of aerosols, this could provide much more efficient $CO_2$ removal rates. There have also been multiple efforts to engineer metabolic pathways in microalgae to enhance photosynthetic efficiency, for example, targeting rubisco expression [54]. However, as recently reviewed by Kim *et al.* (2024), a

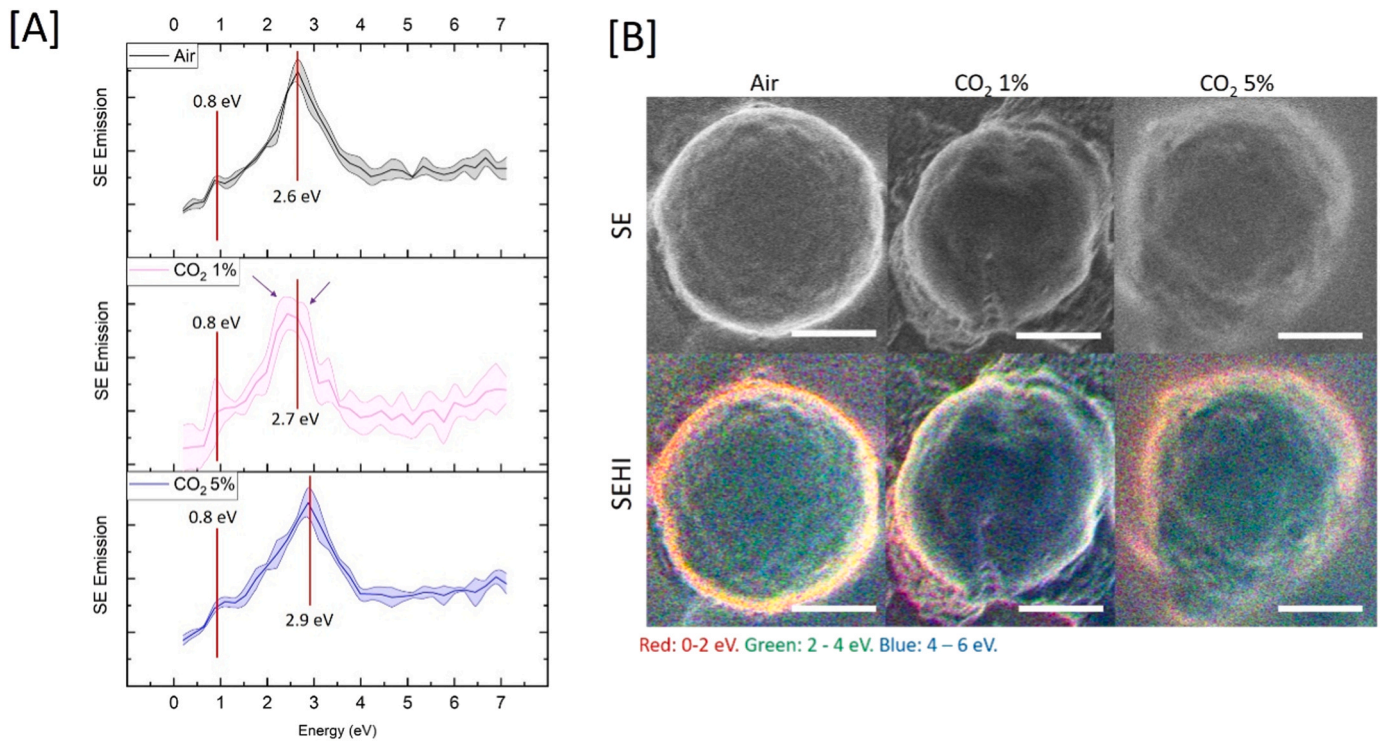


**Fig. 8.** (a) Graphs of secondary electron emission against energy for cells exposed to 0.04, 1 and 5 % (v/v) $CO_2$; (b) SE and SEHI images of cells exposed to 0.04, 1 and 5 % (v/v) $CO_2$. Different energy regimes are attributed to different colours to represent relative intensity.

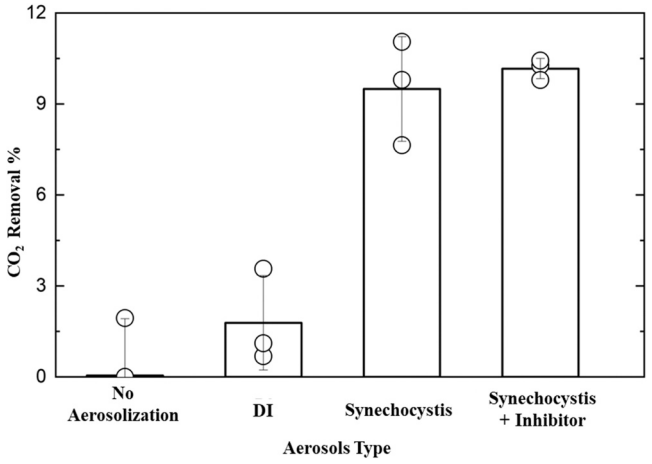


**Fig. 9.** Percentage $CO_2$ removal in varying aerosolization conditions, including a no aerosolization control, deionized water only, *Synechocystis* cells and *Synechocystis* cells with photosynthesis inhibitor, methyl viologen, at the bottom of the well. Triplicate replicate experiments are shown as open circles, with error bars. There is a significant increase in removal percentage (more than 5 fold) for where algae cells were present. However, adding the inhibitor did not reduce the $CO_2$ removal, indicating all $CO_2$ was captured by aerosolized cells.

more logical option could be to optimize carbon flux to specific carbon sinks, leading to improved carbon sequestration and biomass yields [55]. The unique stress conditions produced in an aerosol could also be leveraged to adaptively evolve strains that are able to thrive in such conditions, improving overall efficiencies. In addition, the application of this new technology would need process specific design considerations. For example, it would be suited to where $CO_2$ is omitted over large areas, where concentrations of $CO_2$ are not too high (<1 % v/v), and also where biomass could be captured and perhaps recycled into aerosols. The opportunity to modify current gas scrubbers with biological $CO_2$ removal capability could also be explored.

The wider significance of this research is broad. The novel analytical techniques applied to investigate microalgal health within aerosols can be applied to naturally generated aerosols, where there are implications on atmospheric chemistry [35]. Moreover, the capture of pollutants with this technology need not be restricted to $CO_2$, where applications can extend to other gases including volatile organic compounds.

## 10. Conclusions

This study demonstrates the successful aerosolization of *Synechocystis* cells using a novel batch aerosolization system. Experiments revealed the optimal cell density to perform aerosolization was $1.2 \times 10^8$ cells/mL, and varying concentrations of $CO_2$ had an impact on cell density in the chamber well and pH. Furthermore, the study explored the potential of aerosols containing cyanobacteria to capture $CO_2$ and showed an hourly rate of 3.52 g $CO_2$ removal for every gram of biomass aerosolized. The study also provided insights into the visualization of droplets using static and dynamic methods of imaging, including visible and secondary electron hyperspectral imaging. Spectral analysis showed an increase in cell stress for elevated $CO_2$ levels, critically indicating not to increase the $CO_2$ concentration beyond 1 % to avoid cell stress in this strain. However, using naturally occurring or engineered high $CO_2$ fixing species, or even stress tolerant strains could improve the overall efficiency of the process. The findings of this study provides the very first example of how to aerosolize cyanobacteria cells for $CO_2$ capture, and lays the foundation for further research that can implement the technology at larger scales or integrate with current particulate or gaseous effluent capture methods.

## Funding

We acknowledge our funders, Engineering and Physical Sciences Research Council for two grants, EP/X016951/1 and EP/V012126/1.

## CRediT authorship contribution statement

**Jagroop Pandhal:** Writing – review & editing, Supervision, Funding acquisition, Conceptualization. **Elbaraa Elghazy:** Writing – original draft, Methodology, Investigation, Formal analysis, Data curation. **Nicholas T.H Farr:** Methodology, Data curation, Investigation. **Matt M. J Davies:** Writing – review & editing, Methodology, Investigation, Formal analysis, Data curation. **Jon R. Willmott:** Writing – review & editing, Supervision, Investigation, Funding acquisition, Formal analysis, Conceptualization. **Cornelia Rodenburg:** Writing – review & editing, Methodology, Formal analysis.

## Declaration of Competing Interest

The authors declare the following financial interests/personal relationships which may be considered as potential competing interests: Jagroop Pandhal reports was provided by Engineering and Physical Sciences Research Council. Jagroop Pandhal reports a relationship with Engineering and Physical Sciences Research Council that includes: funding grants. Jagroop Pandhal has patent #2414724.1 pending to Barker Brettell. None. If there are other authors, they declare that they have no known competing financial interests or personal relationships that could have appeared to influence the work reported in this paper.

## Data availability

The data that has been used is confidential.

## References


[1] N. Mac Dowell, P.S. Fennell, N. Shah, G.C. Maitland, The role of CO2 capture and utilization in mitigating climate change, Nat. Clim. Change 7 (4) (2017) 243–249.
[2] S.A. Montzka, E.J. Dlugokencky, J.H. Butler, Non-CO2 greenhouse gases and climate change, Nature 476 (7358) (2011) 43–50.
[3] J.G. Olivier, K.M. Schure, J. Peters, Trends in global CO2 and total greenhouse gas emissions, PBL Neth. Environ. Assess. Agency 5 (2017) 1–11.
[4] K.O. Yoro, M.O. Daramola, CO2 emission sources, greenhouse gases, and the global warming effect. in *Advances in carbon capture*, Elsevier, 2020, pp. 3–28.
[5] K.J. Van Groenigen, C.W. Osenberg, B.A. Hungate, Increased soil emissions of potent greenhouse gases under increased atmospheric CO2, Nature 475 (7355) (2011) 214–216.
[6] Y. Ou, et al., Deep mitigation of CO2 and non-CO2 greenhouse gases toward 1.5° C and 2° C futures,", Nat. Commun. 12 (1) (2021) 6245.
[7] H. Herzog, B. Eliasson, O. Kaarstad, Capturing greenhouse gases, Sci. Am. 282 (2) (2000) 72–79.
[8] S. Lee, J.-W. Choi, S.-H. Lee, Separation of greenhouse gases (SF6, CF4 and CO2) in an industrial flue gas using pilot-scale membrane, Sep. Purif. Technol. 148 (2015) 15–24.
[9] N. Norahim, P. Yaisanga, K. Faungnawakij, T. Charinpanitkul, C. Klaysom, Recent membrane developments for CO2 separation and capture, Chem. Eng. Technol. 41 (2) (2018) 211–223.
[10] A. Lugo, et al., Life cycle energy use and greenhouse gas emissions for a novel algal-osmosis membrane system versus conventional advanced potable water reuse processes: Part I, J. Environ. Manag. 331 (2023) 117293.
[11] A. Bello, D.B. Dorhjie, A. Ivanova, A. Cheremisin, A Numerical Study of the Influence of Rock Mineralization on CO2 Storage. presented at the SPE Gas & Oil Technology Showcase and Conference, SPE, 2023. D021S017R003.
[12] D. Madhav, B. Buffel, F. Desplentere, P. Moldenaers, V. Vandeginste, Bio-inspired mineralization of CO2 into CaCO3: single-step carbon capture and utilization with controlled crystallization, Fuel 345 (2023) 128157.
[13] X. Song, et al., A green approach to preparing vaterite CaCO3 for clean utilization of steamed ammonia liquid waste and CO2 mineralization, Sustainability 15 (17) (2023) 13275.
[14] L. Li, T. Chen, X. Gao, W. Yang, New insights into the effects of different CO2 mineralization conditions on steel slag as supplemental cementitious material, J. Build. Eng. 84 (2024) 108566.
[15] X. Zheng, et al., Bioinspired controllable CaCO3 synthesis from solid waste by an 'all in one' amino acid-in strategy: implication for CO2 mineralization, Chem. Eng. J. 480 (2024) 148037.
[16] Y.-F. Diao, X.-Y. Zheng, B.-S. He, C.-H. Chen, X.-C. Xu, Experimental study on capturing CO2 greenhouse gas by ammonia scrubbing, Energy Convers. Manag. 45 (13–14) (2004) 2283–2296.
[17] M.T. Ravanchi, S. Sahebdelfar, F.T. Zangeneh, Carbon dioxide sequestration in petrochemical industries with the aim of reduction in greenhouse gas emissions, Front. Chem. Sci. Eng. 5 (2) (2011) 173–178.
[18] L.N. Nguyen, et al., Microalgae-based carbon capture and utilization: a critical review on current system developments and biomass utilization, Crit. Rev. Environ. Sci. Technol. 53 (2) (2023) 216–238.
[19] S. Chakurkar, K.G. Guptha, Optimization of cement quantity through the engineering of particle size distribution–a sustainable approach, Results Mater. 19 (2023) 100408.
[20] Y. Guo, et al., A review of low-carbon technologies and projects for the global cement industry, J. Environ. Sci. 136 (2024) 682–697.
[21] S. Raza, Y. Orooji, E. Ghasali, A. Hayat, H. Karimi-Maleh, H. Lin, Engineering approaches for CO2 converting to biomass coupled with nanobiomaterials as biomediated towards circular bioeconomy, J. CO2 Util. 67 (2023) 102295.
[22] M. Sakarika, et al., The nutritional composition and cell size of microbial biomass for food applications are defined by the growth conditions, Microb. Cell Factor. 22 (1) (2023) 254.
[23] Y.M. Bar-On, R. Milo, The biomass composition of the oceans: a blueprint of our blue planet, Cell 179 (7) (2019) 1451–1454.
[24] R.L. Chapman, Algae: the world's most important 'plants'—an introduction, Mitig. Adapt. Strateg. Glob. Change 18 (2013) 5–12.
[25] M. Shahabuddin, G. Brooks, M.A. Rhamdhani, Decarbonisation and hydrogen integration of steel industries: Recent development, challenges and technoeconomic analysis, J. Clean. Prod. 395 (2023) 136391.
[26] J. Zhang, J. Shen, L. Xu, Q. Zhang, The CO2 emission reduction path towards carbon neutrality in the Chinese steel industry: a review, Environ. Impact Assess. Rev. 99 (2023) 107017.
[27] S.A. Razzak, et al., Microalgae cultivation in photobioreactors: sustainable solutions for a greener future, Green. Chem. Eng. (2023).
[28] J.A. Raven, J. Beardall, The ins and outs of CO2, J. Exp. Bot. 67 (1) (2016) 1–13.
[29] S. Dey, A. Bhattacharya, P. Kumar, A. Malik, High-rate CO 2 sequestration using a novel venturi integrated photobioreactor and subsequent valorization to microalgal lipids, Green. Chem. 22 (22) (2020) 7962–7973.
[30] W.B. Zimmerman, M. Zandi, H.H. Bandulasena, V. Tesař, D.J. Gilmour, K. Ying, Design of an airlift loop bioreactor and pilot scales studies with fluidic oscillator induced microbubbles for growth of a microalgae Dunaliella salina, Appl. Energy 88 (10) (2011) 3357–3369.
[31] P. In-na, A.A. Umar, A.D. Wallace, M.C. Flickinger, G.S. Caldwell, J.G.M. Lee, Loofah-based microalgae and cyanobacteria biocomposites for intensifying carbon dioxide capture, J. CO2 Util. 42 (Dec. 2020) 101348, https://doi.org/10.1016/j.jcou.2020.101348.
[32] K. Wiśniewska, A.U. Lewandowska, S. Śliwińska-Wilczewska, The importance of cyanobacteria and microalgae present in aerosols to human health and the environment – review study, Environ. Int. 131 (Oct. 2019) 104964, https://doi.org/10.1016/j.envint.2019.104964.
[33] Y.-L. Pan, A. Kalume, C. Wang, J. Santarpia, Atmospheric aging processes of bioaerosols under laboratory-controlled conditions: a review, J. Aerosol Sci. 155 (Jun. 2021) 105767, https://doi.org/10.1016/j.jaerosci.2021.105767.
[34] N.I. Medina-Pérez, M. Dall'Osto, S. Decesari, M. Paglione, E. Moyano, E. Berdalet, Aerosol toxins emitted by harmful algal blooms susceptible to complex air–sea interactions, Environ. Sci. Technol. 55 (1) (Jan. 2021) 468–477, https://doi.org/10.1021/acs.est.0c05795.
[35] S.V. Tesson, C.A. Skjøth, T. Šantl-Temkiv, J. Löndahl, Airborne microalgae: insights, opportunities, and challenges, Appl. Environ. Microbiol. 82 (7) (2016) 1978–1991.
[36] W. Tang, et al., Widespread phytoplankton blooms triggered by 2019–2020 Australian wildfires, Art. no. 7876, Nature 597 (7876) (Sep. 2021), https://doi.org/10.1038/s41586-021-03805-8.
[37] S. Anand, K. Rykaczewski, S.B. Subramanyam, D. Beysens, K.K. Varanasi, How droplets nucleate and grow on liquids and liquid impregnated surfaces, Soft Matter 11 (1) (Jan. 2015) 69–80, https://doi.org/10.1039/c4sm01424c.
[38] M.B. Stuart, M. Davies, M.J. Hobbs, T.D. Pering, A.J.S. McGonigle, J.R. Willmott, High-resolution hyperspectral imaging using low-cost components: application within environmental monitoring scenarios, Sensors 22 (12) (2022) 4652.
[39] M.B. Stuart, M. Davies, M.J. Hobbs, A.J.S. McGonigle, J.R. Willmott, Peatland plant spectral response as a proxy for peat health, analysis using low-cost hyperspectral imaging techniques, Remote Sens. 14 (16) (2022) 3846.
[40] P.J. Zarco-Tejada, et al., Assessing vineyard condition with hyperspectral indices: leaf and canopy reflectance simulation in a row-structured discontinuous canopy, Remote Sens. Environ. 99 (3) (Nov. 2005) 271–287, https://doi.org/10.1016/j.rse.2005.09.002.
[41] J. Chen, H. Xu, Analysis of the effectiveness of the red-edge bands of GF-6 imagery in forest health discrimination, IEEE J. Sel. Top. Appl. Earth Obs. Remote Sens. 17 (2024) 5621–5636, https://doi.org/10.1109/JSTARS.2024.3367320.
[42] N. Farr, et al., Understanding surface modifications induced via argon plasma treatment through secondary electron hyperspectral imaging, Adv. Sci. 8 (4) (2021) 2003762, https://doi.org/10.1002/advs.202003762.
[43] N. Farr, S. Pashneh-Tala, N. Stehling, F. Claeyssens, N. Green, C. Rodenburg, Characterizing cross-linking within polymeric biomaterials in the SEM by secondary electron hyperspectral imaging, Macromol. Rapid Commun. 41 (3) (2020) 1900484, https://doi.org/10.1002/marc.201900484.
[44] Y. Takaku, S. Takehara, C. Suzuki, H. Suzuki, M. Shimomura, T. Hariyama, In situ elemental analyses of living biological specimens using 'NanoSuit' and EDS methods in FE-SEM, Sci. Rep. 10 (1) (Sep. 2020) 14574, https://doi.org/10.1038/s41598-020-71523-8.
[45] N.T.H. Farr, Revealing localised mechanochemistry of biomaterials using in situ multiscale chemical analysis, Materials 15 (10) (2022) 3462.
[46] J.F. Nohl, N.T.H. Farr, Y. Sun, G.M. Hughes, S.A. Cussen, C. Rodenburg, Low-voltage SEM of air-sensitive powders: from sample preparation to micro/nano

analysis with secondary electron hyperspectral imaging, Micron 156 (May 2022) 103234, https://doi.org/10.1016/j.micron.2022.103234.
[47] D. Li, L. Wang, Q. Zhao, W. Wei, Y. Sun, Improving high carbon dioxide tolerance and carbon dioxide fixation capability of Chlorella sp. by adaptive laboratory evolution, Bioresour. Technol. 185 (Jun. 2015) 269–275, https://doi.org/10.1016/j.biortech.2015.03.011.
[48] B. Barati, F.F. Zafar, L. Qian, S. Wang, A.E.-F. Abomohra, Bioenergy characteristics of microalgae under elevated carbon dioxide, Fuel 321 (2022) 123958.
[49] P. Varshney, J. Beardall, S. Bhattacharya, P.P. Wangikar, Effect of elevated carbon dioxide and nitric oxide on the physiological responses of two green algae, Asterarcys quadricellulare and Chlorella sorokiniana, J. Appl. Phycol. 32 (1) (Feb. 2020) 189–204, https://doi.org/10.1007/s10811-019-01950-2.
[50] J. Smarda, D. Smajs, J. Komrska, V. Krzyzánek, S-layers on cell walls of cyanobacteria, 77, Micron 33 (3) (2002) 257, https://doi.org/10.1016/s0968-4328(01)00031-2.
[51] J. Han, D.A. Eimer, M.C. Melaaen, Liquid phase mass transfer coefficient of carbon dioxide absorption by water droplet, Energy Procedia 37 (2013) 1728–1735, https://doi.org/10.1016/j.egypro.2013.06.048.
[52] H. Leflay, J. Pandhal, S. Brown, Direct measurements of CO2 capture are essential to assess the technical and economic potential of algal-CCUS, J. CO2 Util. 52 (Oct. 2021) 101657, https://doi.org/10.1016/j.jcou.2021.101657.
[53] A. Włodarczyk, T.T. Selão, B. Norling, P.J. Nixon, Newly discovered Synechococcus sp. PCC 11901 is a robust cyanobacterial strain for high biomass production, Commun. Biol. 3 (1) (May 2020) 215, https://doi.org/10.1038/s42003-020-0910-8.
[54] "Synechocystis PCC 6803 overexpressing RuBisCO grow faster with increased photosynthesis - ScienceDirect." Accessed: Nov. 27, 2024. [Online]. Available: ⟨https://www.sciencedirect.com/science/article/pii/S2214030116300402?via%3Dihub⟩.
[55] D.S. Kim, J.Á. Moreno-Cabezuelo, E.N. Schulz, D.J. Lea-Smith, U.S. Sagaram, Recent advances in engineering fast-growing cyanobacterial species for enhanced CO2 fixation, Front. Clim. 6 (Jun. 2024), https://doi.org/10.3389/fclim.2024.1412232.